Supporting Information for

Circular Dichroisms of Mono- and Dibromo[2.2]paracyclophanes. A Combined Experimental and Theoretical Study

Mitsunobu Toda, Yoshihisa Inoue, and Tadashi Mori*

Department of Applied Chemistry, Graduate School of Engineering, Osaka University, 2-1 Yamada-oka, Suita, Osaka, 565-0871, Japan

Contents

1. General experimental details (page S3).
2. HPLC traces for enantiomeric separation of brominated [2.2]paracyclophanes (Figures S1-S4, pages S4-S5).
3. Experimental UV/CD spectra and *g* factors of brominated [2.2]paracyclophanes (Figures S5-S7, pages S6-S8).
4. Calculated CD spectra with rotatory strengths of brominated [2.2]paracyclophanes (Figure S8, page S9).
5. Comparison of calculated CD spectra with different theoretical methods (Figure S9, page S10).
6. Potential energy profile against the twist angle in 4-bromo[2.2]paracyclophane (Figure S10, page S11).
7. Optimized geometries of brominated [2.2]paracyclophanes (Table S1, pages S12-S13).

General Experimental Details

UV-vis spectra were obtained on JASCO V-550 or 560 equipped with a PTC-348WI temperature controller under the following conditions: bandwidth, 2 nm; scan rate, 100 nm min^{-1}; response, medium. Electronic circular dichroism (CD) spectra were measured in a conventional quartz cell (light path length: 1 cm) on a J-720WI spectropolarimeter equipped with a PTC-505T temperature controller under the following conditions: bandwidth, 2 nm; scan rate, 100 nm min^{-1}, response, 4 sec; accumulation, 4 times. Concentration of sample solutions was set to $2\sim3 \times 10^{-5}$ M in acetonitrile.

All calculations were performed on Linux-PCs by using Gaussian 09[S1] or TURBOMOLE 7.2[S2] program suite. Geometries were fully optimized at the dispersion-corrected density functional theory with AO basis-set of valence triple-ξ quality at the DFT-D3(BJ)-TPSS/def2-TZVPP level.[S3] The resolution of identity (RI) approximation was employed and the corresponding auxiliary basis-sets were taken from the Turbomole basis-set library. The numerical quadrature grid m5 was employed and the convergence criterion for the optimization regarding the change of total energy between two subsequent optimization cycles was set to 10^{-7} E_h. All excited-state calculations were performed with the above DFT-D3 optimized ground-state geometries, thus corresponding to the vertical transition approximation. The CD spectrum was calculated by the time-dependent, second-order approximate coupled-cluster singles and doubles model (RI-CC2 method)[S4] and by the algebraic diagrammatic construction scheme that combines perturbation theory with configuration interaction (RI-ADC(2) method),[S5] both in conjunction with the resolution-of-identity method using the def2-TZVPP basis-sets. The calculated rotational strengths in length gauge were expanded by Gaussian functions and overlapped where the width of the band at 1/e height is fixed at 0.4 eV, with energy shift of 0.2 eV and scaling of 3~5 to facilitate direct comparison with experiment. The rotational strengths were also verified by the SAC-CI and TD-DFT methods for comparison purpose. Numerical values presented in Table 3 were not corrected.

(S1) Gaussian 09, Revision D.01, Frisch, M. J.; Trucks, G. W.; Schlegel, H. B.; Scuseria, G. E.; Robb, M. A.; Cheeseman, J. R.; Scalmani, G.; Barone, V.; Mennucci, B.; Petersson, G. A.; Nakatsuji, H.; Caricato, M.; Li, X.; Hratchian, H. P.; Izmaylov, A. F.; Bloino, J.; Zheng, G.; Sonnenberg, J. L.; Hada, M.; Ehara, M.; Toyota, K.; Fukuda, R.; Hasegawa, J.; Ishida, M.; Nakajima, T.; Honda, Y.; Kitao, O.; Nakai, H.; Vreven, T.; Montgomery, J. A., Jr.; Peralta, J. E.; Ogliaro, F.; Bearpark, M.; Heyd, J. J.; Brothers, E.; Kudin, K. N.; Staroverov, V. N.; Kobayashi, R.; Normand, J.; Raghavachari, K.; Rendell, A.; Burant, J. C.; Iyengar, S. S.; Tomasi, J.; Cossi, M.; Rega, N.; Millam, J. M.; Klene, M.; Knox, J. E.; Cross, J. B.; Bakken, V.; Adamo, C.; Jaramillo, J.; Gomperts, R.; Stratmann, R. E.; Yazyev, O.; Austin, A. J.; Cammi, R.; Pomelli, C.; Ochterski, J. W.; Martin, R. L.; Morokuma, K.; Zakrzewski, V. G.; Voth, G. A.; Salvador, P.; Dannenberg, J. J.; Dapprich, S.; Daniels, A. D.; Farkas, Ö.; Foresman, J. B.; Ortiz, J. V.; Cioslowski, J.; Fox, D. J. Gaussian, Inc., Wallingford CT, 2009.

(S2) Turbomole V7.2 2017, a development of University of Karlsruhe and Forschungszentrum Karlsruhe GmbH, 1989-2007, Turbomole GmbH, since 2007; available from http://www.turbomole.com.

(S3) (a) Grimme, S.; Antony, J.; Ehrlich, S.; Krieg, H. A Consistent and Accurate Ab Initio Parametrization of Density Functional Dispersion Correction (DFT-D) for the 94 Elements H-Pu. *J. Chem. Phys.* **2010**, *132*, 154104/1-18. (b) Grimme, S.; Ehrlich, S.; Goerigk, L. Effect of the Damping Function in Dispersion Corrected Density Functional Theory. *J. Comput. Chem.* **2011**, *32*, 1456-1465. (c) Tao, J.; Perdew, J. P.; Staroverov, V. N.; Scuseria, G. E. Climbing the Density Functional Ladder: Nonempirical Meta-Generalized Gradient Approximation Designed for Molecules and Solids. *Phys. Rev. Lett.* **2003**, *91*, 146401/1-4.

(S4) Christiansen, R.; Koch, H.; Jørgensen, P. The Second-Order Approximate Coupled Cluster Singles and Doubles Model CC2. *Chem. Phys. Lett.* **1995**, *243*, 409-418. (a) Hättig, C.; Weigend, F. CC2 Excitation Energy Calculations on Large Molecules Using the Resolution of the Identity Approximation. *J. Chem. Phys.* **2000**, *113*, 5154-5161. (b) Hättig, C.; Kohn, A. Transition Moments and Excited-State First-Order Properties in the Coupled-Cluster Model CC2 Using the Resolution-of-the-Identity Approximation. *J. Chem. Phys.* **2002**, *117*, 6939-6951.

(S5) Hättig, C. Structure Optimizations for Excited States with Correlated Second-Order Methods: CC2, CIS(D1), and ADC(2). *Adv. Quant. Chem.* **2005**, *50*, 37-60.

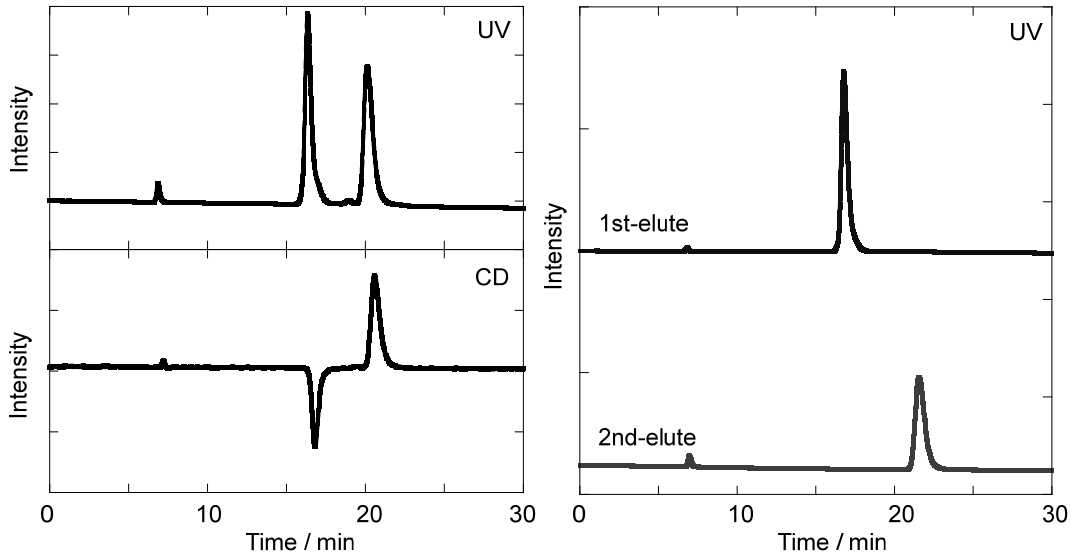

Figure S1. HPLC traces for the enantiomer separation of 4-bromoparacyclophane **1**. Conditions: column, Daicel Chiralcel IA (4.6 mm φ × 25 cm); eluent, hexane : dichloromethane = 99 : 1; flow rate, 0.5 mL min^{-1}; pressure, 1.3 MPa; temperature, 35 °C; UV and CD detector, monitored at 254 nm. Right panel shows the successful optical resolution of both enantiomers (R_s = 4.3).

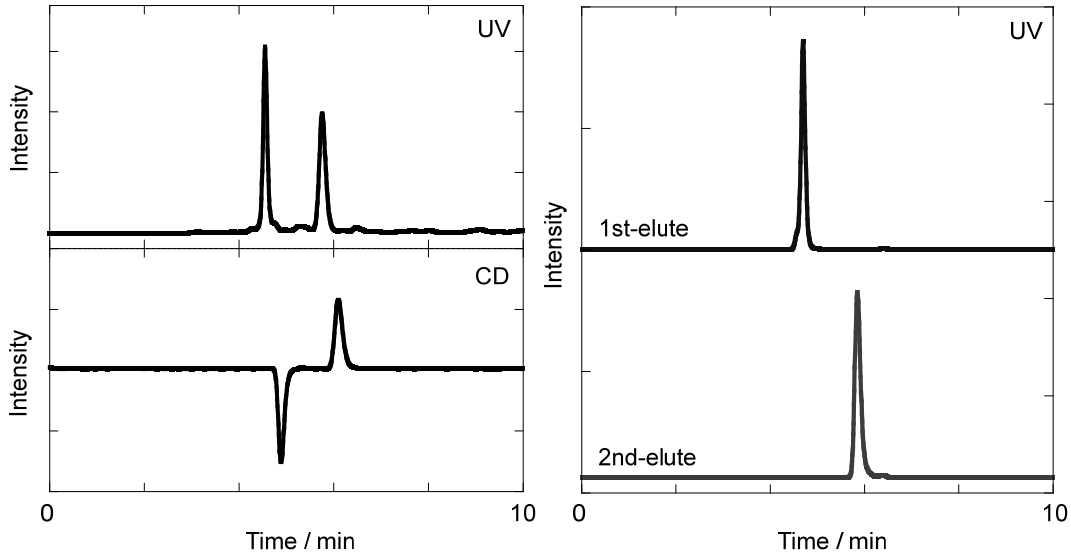

Figure S2. HPLC traces for the enantiomer separation of *para*- or 4,7-dibromoparacyclophane *p*-**2**. Conditions: column, Daicel Chiralcel IA (4.6 mm φ × 25 cm); eluent, hexane : 2-propanol = 99 : 1; flow rate, 0.5 mL min^{-1}; pressure, 1.3 MPa; temperature, 35 °C; UV and CD detector, monitored at 254 nm. Right panel shows the successful optical resolution of both enantiomers (R_s = 8.5).

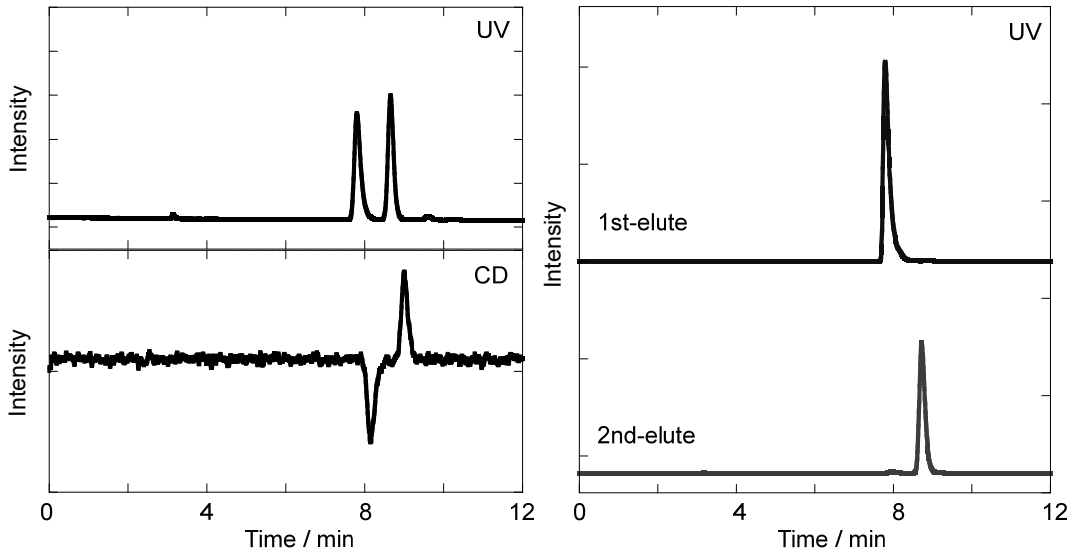

Figure S3. HPLC traces for the enantiomer separation of *pseudo-meta*- or 4,15-dibromoparacyclophane *m'*-**2**. Conditions: column, Daicel Chiralpak OD-3 (4.6 mm φ × 25 cm); eluent, hexane : dichloromethane = 99 : 1; flow rate, 1.0 mL min^{-1}; pressure, 2.6 MPa; temperature, 35 °C; UV and CD detector, monitored at 254 nm. Right panel shows the successful optical resolution of both enantiomers (R_s = 3.0).

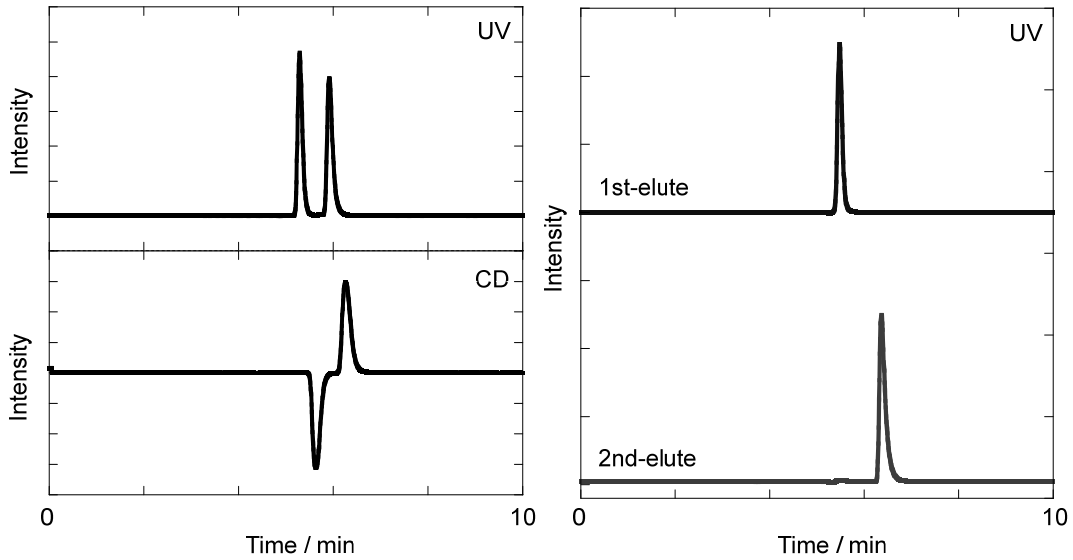

Figure S4. HPLC traces for the enantiomer separation of *pseudo-ortho*- or 4,12-dibromoparacyclophane *o'*-**2**. Conditions: column, Daicel Chiralcel IB (4.6 mm φ × 25 cm); eluent, hexane : 2-propanol = 99 : 1; flow rate, 1.0 mL min^{-1}; pressure, 2.6 MPa; temperature, 35 °C; UV and CD detector, monitored at 254 nm. Right panel shows the successful optical resolution of both enantiomers (R_s = 2.1).

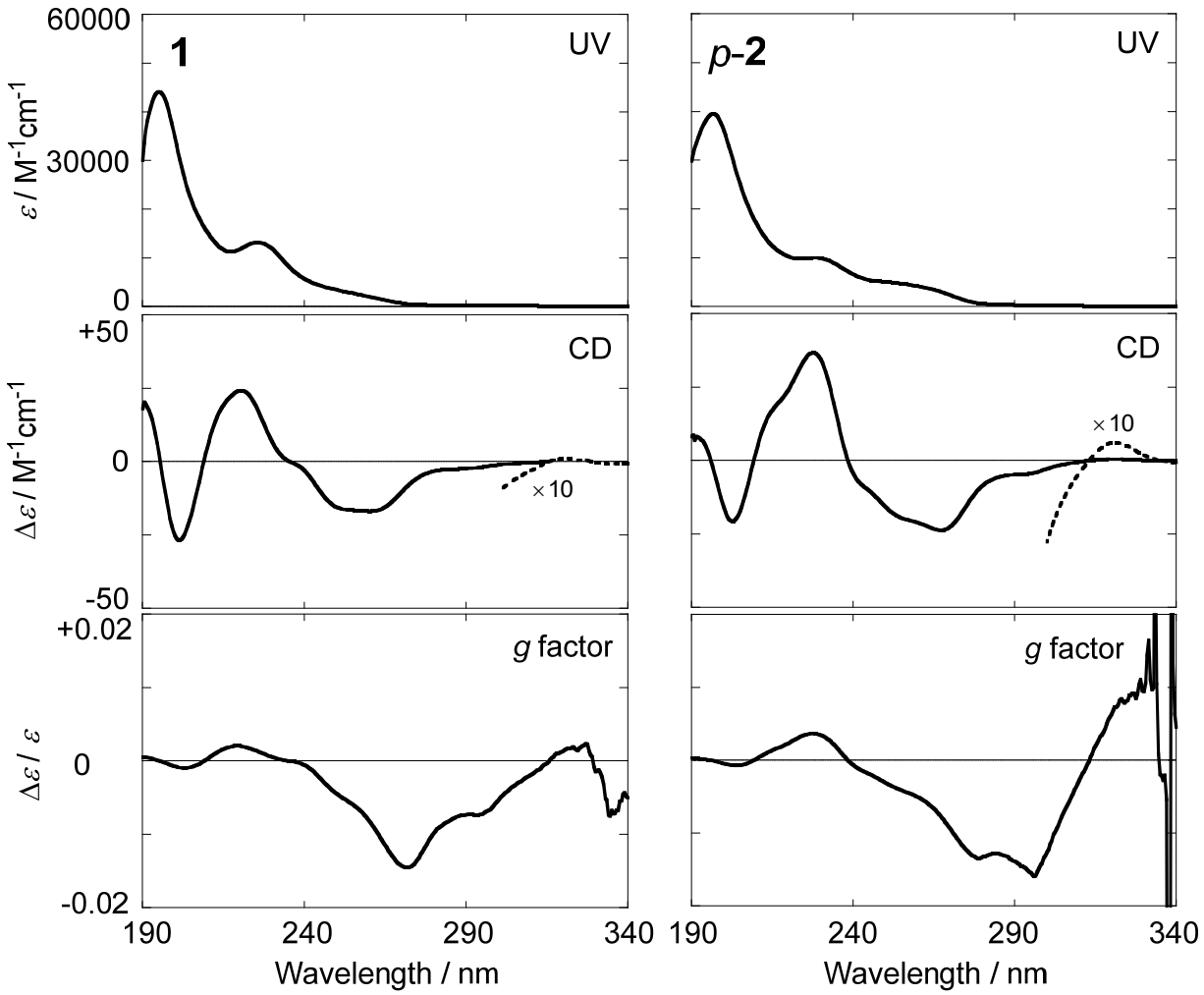

Figure S5. Experimental UV (top) and CD spectra (middle) and anisotropy (*g*) factor profiles (bottom) of **1** (left) and *p*-**2** (right) of 1st elutes from chiral HPLC in acetonitrile at 25 °C.

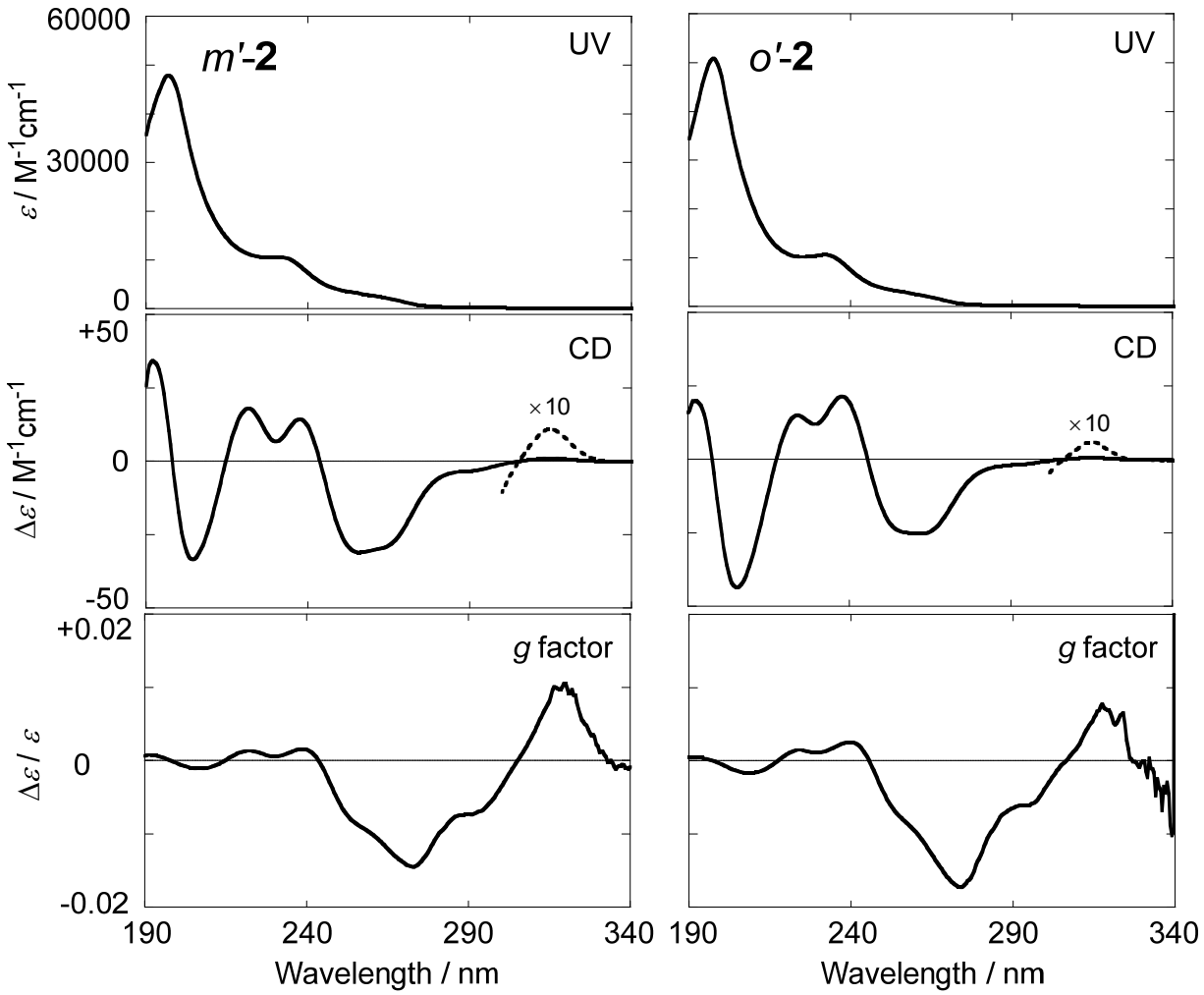

Figure S6. Experimental UV (top) and CD spectra (middle) and anisotropy (*g*) factor profiles (bottom) of *m'*-**2** (left) and *o'*-**2** (right) of 1st elutes from chiral HPLC in acetonitrile at 25 °C.

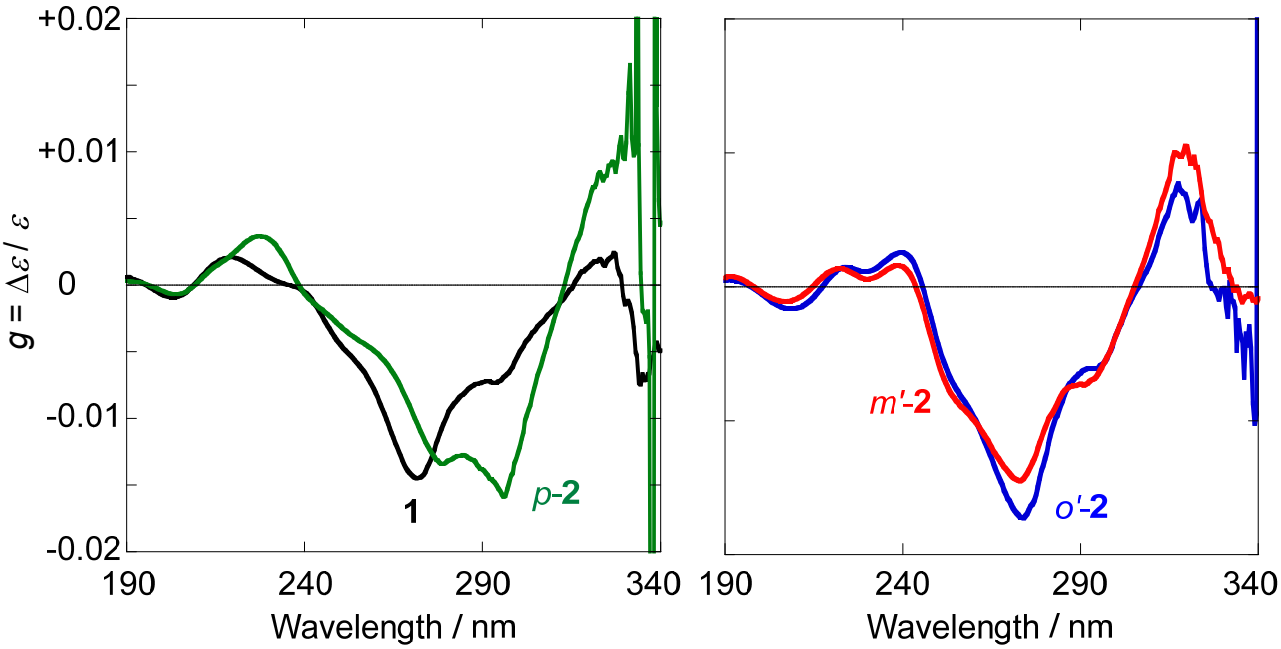

Figure S7. Comparison of anisotropy (*g*) factor profiles between **1** and *p*-**2** and between *m'*-**2** and *o'*-**2**.

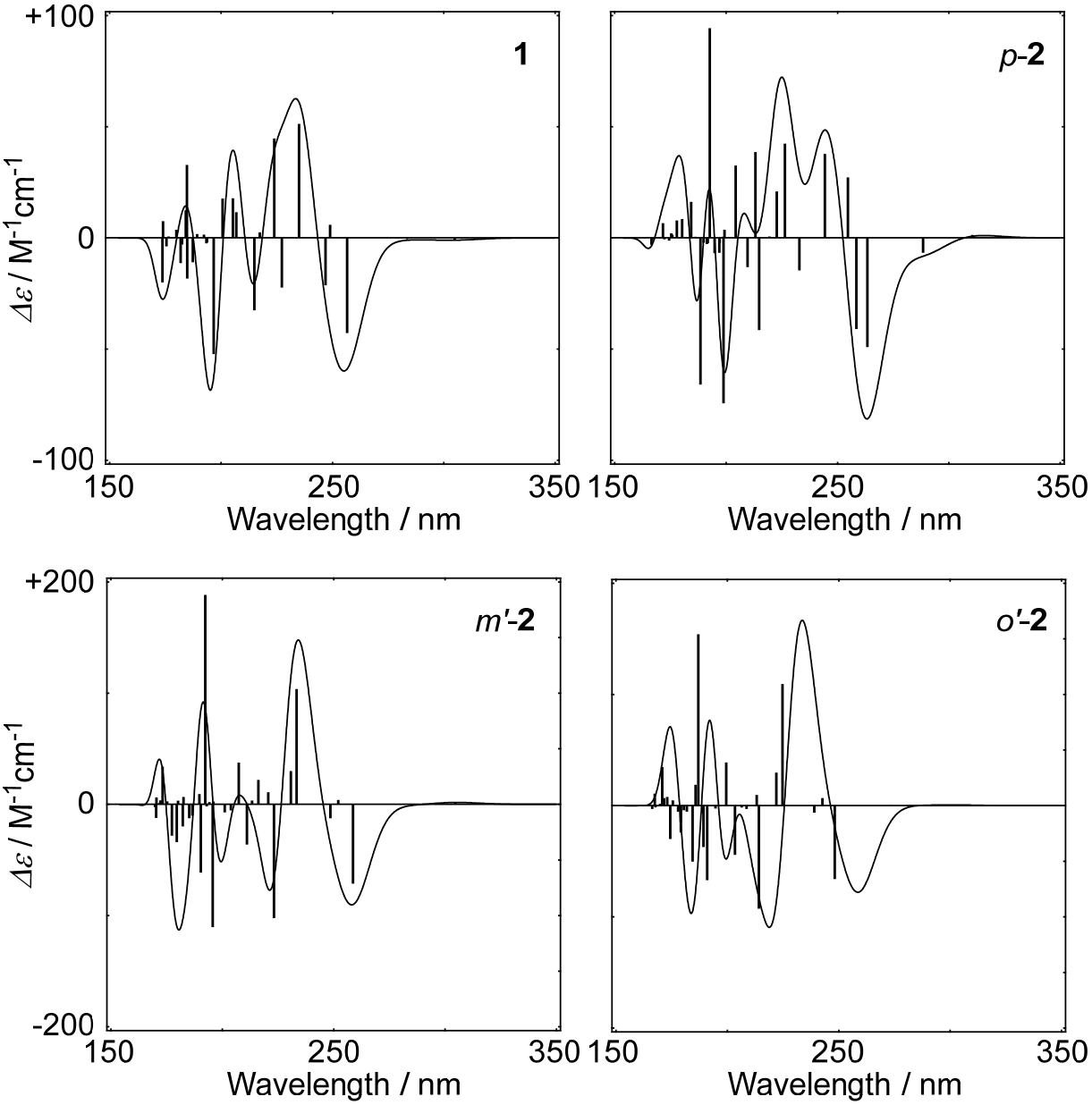

Figure S8. Calculated CD spectra and rotatory strengths (in bar representation) of brominated [2.2]paracyclophanes **1**-**2** at the RI-CC2/def2-TZVPP level. Spectra were not shifted or scaled.

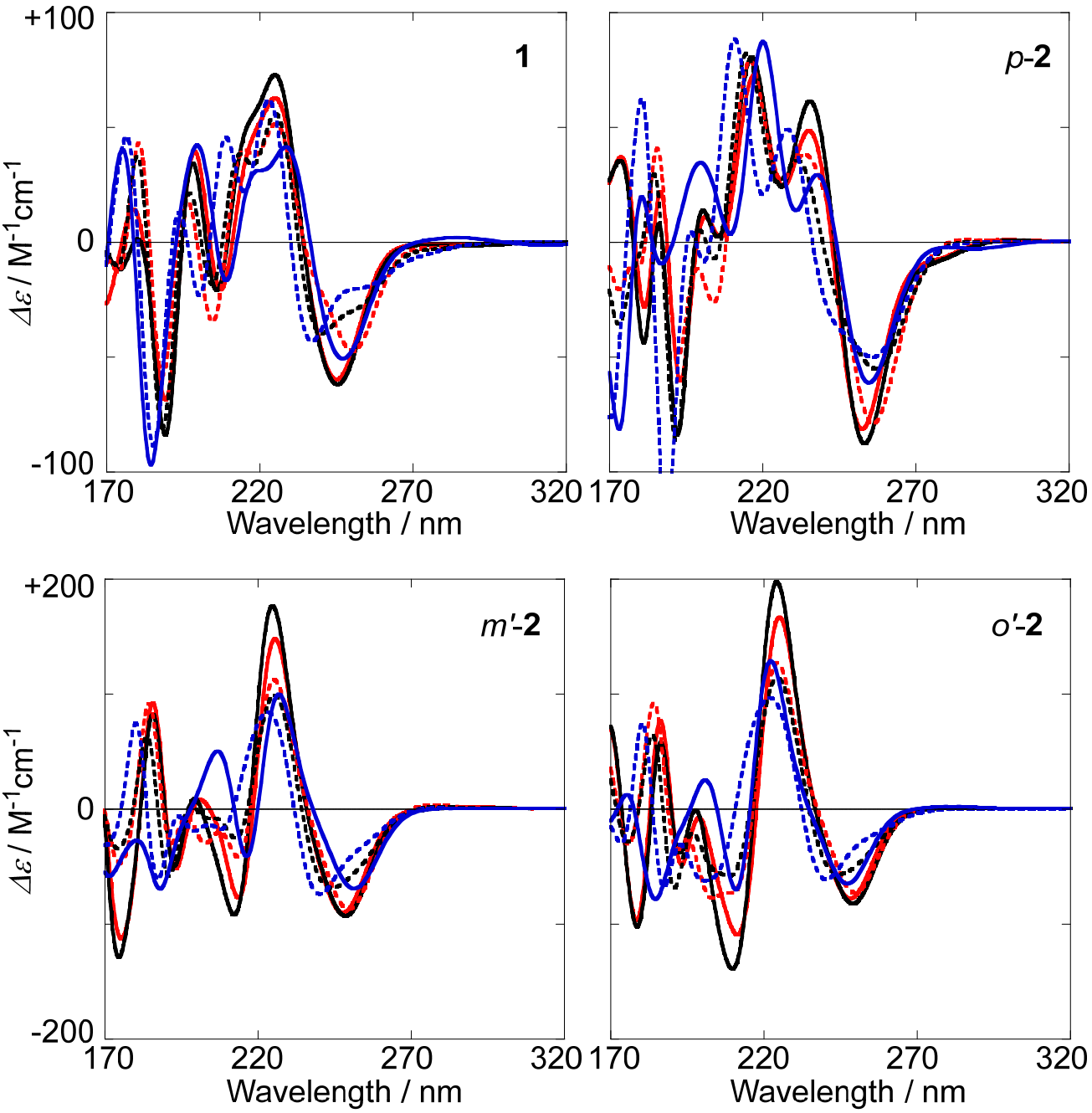

Figure S9. Comparison of calculated CD spectra of brominated [2.2]paracyclophanes **1**-**2** by different theoretical methods. Red solid: RI-CC2/def2-TZVPP, black solid: RI-ADC(2)/def2-TZVPP, blue solid: SAC-CI/def2-TZVP, red dotted: TD-DFT-M06-2X/def2-TZVP, black dotted: TD-DFT-CAM-B3LYP/def2-TZVP blue dotted: TD-DFT-BHLYP/def2-TZVP. Spectra of SAC-CI method were 0.8 eV blue-shifted for comparison. Other spectra were not shifted or scaled.

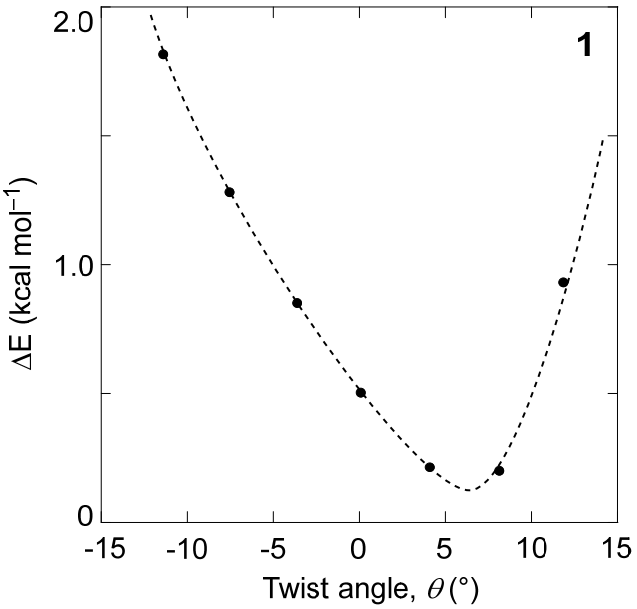

Figure S10. Potential energy curve for **1** as a function of twist angle θ. Relative energies in the gas phase calculated at the SCS-MP2/TZVPP//DFT-D3(BJ)-TPSS/def2-TZVP level.

TABLE S1. Optimized Geometries of Bromo[2.2]paracyclophanes at the DFT-D3-TPSS/def2-TZVPP Level.

1 (4-bromo[2.2]paracyclophane)

Br	3.545642	0.401992	-0.069236
C	-0.999034	-1.680323	0.632563
C	0.333919	-1.631475	1.059289
C	0.703447	-0.555540	1.877875
C	-0.122726	0.559666	2.006555
C	-1.342387	0.625226	1.321462
C	-1.823334	-0.564951	0.759515
C	-0.003878	-0.498659	-2.035265
C	1.228902	-0.681899	-1.390751
C	1.784215	0.471659	-0.825733
C	1.042433	1.631431	-0.627793
C	-0.298389	1.682205	-1.028156
C	-0.757659	0.659052	-1.865711
C	1.391922	-2.508162	0.429970
C	1.719421	-2.073632	-1.077885
C	-1.249060	2.625700	-0.332350
C	-1.963087	1.947795	0.941135
H	0.249874	1.437536	2.529133
H	-2.805643	-0.574479	0.293176
H	-0.442714	-1.345794	-2.556275
H	1.466800	2.439861	-0.041742
H	-1.767883	0.699014	-2.263972
H	1.089092	-3.559957	0.406647
H	2.312978	-2.439259	1.014049
H	2.798176	-2.168532	-1.227855
H	1.224400	-2.773795	-1.756407
H	-2.033409	2.968663	-1.013653
H	-0.702901	3.508335	0.012072
H	-1.912611	2.663023	1.767726
H	-3.019217	1.800574	0.697428
H	1.705212	-0.525921	2.297215
H	-1.352504	-2.539355	0.066977

***p*-2 (4,7-dibromo[2.2]paracyclophane)**

Br	-3.272567	0.264516	1.533614
Br	3.272567	-0.264516	1.533614
C	0.490356	-1.295780	-1.536489
C	-0.887680	-1.097266	-1.384356
C	-1.365808	0.211510	-1.535930
C	-0.490356	1.295780	-1.536489
C	0.887680	1.097266	-1.384356
C	1.365808	-0.211510	-1.535930
C	0.601993	-1.240199	1.533114
C	-0.790928	-1.185465	1.385708
C	-1.367467	0.079352	1.547844
C	-0.601993	1.240199	1.533114
C	0.790928	1.185465	1.385708
C	1.367467	-0.079352	1.547844
C	-1.777400	-2.163193	-0.787605
C	-1.518379	-2.360383	0.781553
C	1.518379	2.360383	0.781553
C	1.777400	2.163193	-0.787605
H	-0.896724	2.304276	-1.512508
H	2.436762	-0.392906	-1.508537
H	1.099881	-2.202908	1.487662
H	-1.099881	2.202908	1.487662
H	-1.626270	-3.136396	-1.265246
H	-2.823944	-1.881301	-0.927391
H	-2.483487	-2.531015	1.265361
H	-0.908015	-3.255982	0.924198
H	2.483487	2.531015	1.265361
H	0.908015	3.255982	0.924198
H	1.626270	3.136396	-1.265246
H	2.823944	1.881301	-0.927391
H	-2.436762	0.392906	-1.508537
H	0.896724	-2.304276	-1.512508

m'-**2 (4,15-dibromo[2.2]paracyclophane)**

Br	-3.140261	0.211384	-1.664956
Br	3.140261	-0.211384	-1.664956
C	1.751062	0.697576	-0.703252
C	0.654772	1.218404	-1.400079
C	-0.235764	1.984207	-0.631654
C	-0.203883	1.965779	0.760487
C	0.734536	1.176360	1.435826
C	1.796871	0.656706	0.686268
C	0.235764	-1.984207	-0.631654
C	-0.654772	-1.218404	-1.400079
C	-1.751062	-0.697576	-0.703252
C	-1.796871	-0.656706	0.686268
C	-0.734536	-1.176360	1.435826
C	0.203883	-1.965779	0.760487
C	0.260248	0.756471	-2.781604
C	-0.260248	-0.756471	-2.781604
C	-0.476708	-0.648967	2.826211
C	0.476708	0.648967	2.826211
H	-0.999958	2.454068	1.316006
H	2.592350	0.105336	1.176487
H	1.061367	-2.475721	-1.137971
H	-2.592350	-0.105336	1.176487
H	0.999958	-2.454068	1.316006
H	1.093067	0.818655	-3.487152
H	-0.543814	1.399696	-3.145842
H	-1.093067	-0.818655	-3.487152
H	0.543814	-1.399696	-3.145842
H	-0.004357	-1.411557	3.451983
H	-1.423370	-0.373638	3.299241
H	0.004357	1.411557	3.451983
H	1.423370	0.373638	3.299241
H	-1.061367	2.475721	-1.137971

o'-**2 (4,12-dibromo[2.2]paracyclophane)**

Br	-3.366247	1.211868	-0.008964
Br	-1.810387	-3.058253	0.416061
C	0.913178	0.629357	-1.787561
C	-0.046588	-0.376294	-1.953151
C	-1.353168	-0.095410	-1.534416
C	-1.600218	1.013389	-0.730197
C	-0.577776	1.865874	-0.298395
C	0.645623	1.724055	-0.971118
C	1.713003	-0.882785	0.785667
C	0.773482	-1.796091	0.283054
C	-0.484935	-1.757083	0.894220
C	-0.882279	-0.701798	1.710145
C	-0.001912	0.359028	1.956911
C	1.341880	0.174909	1.610308
C	0.343699	-1.801934	-2.266175
C	1.043962	-2.516265	-1.014709
C	-0.557229	1.725810	2.282878
C	-0.644266	2.658765	0.983340
H	1.449498	2.414232	-0.728005
H	2.728291	-0.924092	0.399428
H	-1.916976	-0.634736	2.027597
H	2.074284	0.939007	1.856680
H	1.040639	-1.856454	-3.108215
H	-0.549172	-2.372445	-2.532678
H	0.697437	-3.552599	-0.985311
H	2.124156	-2.528183	-1.183776
H	0.057917	2.248218	3.022040
H	-1.562187	1.619579	2.698093
H	-1.565315	3.243295	1.053374
H	0.197856	3.355906	1.001607
H	-2.146225	-0.814320	-1.708219
H	1.919974	0.485450	-2.170515